

available at www.sciencedirect.comjournal homepage: www.elsevier.com/locate/biochempharm

In vitro hepatic conversion of the anticancer agent nemorubicin to its active metabolite PNU-159682 in mice, rats and dogs: A comparison with human liver microsomes

Luigi Quintieri^a, Marianna Fantin^a, Pietro Palatini^a, Sara De Martin^a, Antonio Rosato^{b,c}, Michele Caruso^d, Cristina Geroni^e, Maura Floreani^{a,*}

^a Department of Pharmacology and Anaesthesiology, University of Padova, Largo Meneghetti 2, 35131 Padova, Italy

^b Department of Oncology and Surgical Sciences, University of Padova, Padova, Italy

^c Istituto Oncologico Veneto (IOV), Padova, Italy

^d Department of Chemistry, Nerviano Medical Sciences S.r.l., Nerviano, Italy

^e Department of Cell Biology, Oncology, Nerviano Medical Sciences S.r.l., Nerviano, Italy

ARTICLE INFO

Article history:

Received 10 June 2008

Accepted 1 July 2008

Keywords:

Nemorubicin oxidative metabolism

PNU-159682

Liver microsomes

CYP3A enzymes

Sex- and species-related differences

ABSTRACT

We recently demonstrated that nemorubicin (MMDX), an investigational antitumor drug, is converted to an active metabolite, PNU-159682, by human liver cytochrome P450 (CYP) 3A4. The objectives of this study were: (1) to investigate MMDX metabolism by liver microsomes from laboratory animals (mice, rats, and dogs of both sexes) to ascertain whether PNU-159682 is also produced in these species, and to identify the CYP form(s) responsible for its formation; (2) to compare the animal metabolism of MMDX with that by human liver microsomes (HLMs), in order to determine which animal species is closest to human beings; (3) to explore whether differences in PNU-159682 formation are responsible for previously reported species- and sex-related differences in MMDX host toxicity.

The animal metabolism of MMDX proved to be qualitatively similar to that observed with HLMs since, in all tested species, MMDX was mainly converted to PNU-159682 by a single CYP3A form. However, there were marked quantitative inter- and intra-species differences in kinetic parameters. The mouse and the male rat exhibited V_{max} and intrinsic metabolic clearance (CL_{int}) values closest to those of human beings, suggesting that these species are the most suitable animal models to investigate MMDX biotransformation. A close inverse correlation was found between MMDX CL_{int} and previously reported values of MMDX LD_{50} for animals of the species, sex and strain tested here, indicating that differences in the *in vivo* toxicity of MMDX are most probably due to sex- and species-related differences in the extent of PNU-159682 formation.

© 2008 Elsevier Inc. All rights reserved.

1. Introduction

The search for less toxic and more effective anthracyclines has led to the discovery of nemorubicin (3'-deamino-3'-[2''(S)-

methoxy-4''-morpholinyl]doxorubicin; MMDX), a doxorubicin derivative in which the amino nitrogen of the daunosamine unit is incorporated into a methoxymorpholinyl ring (Fig. 1) [1,2]. Early preclinical investigations showed that MMDX,

* Corresponding author. Tel.: +39 049 827 5088; fax: +39 049 827 5093.

E-mail address: m.floreani@unipd.it (M. Floreani).

0006-2952/\$ – see front matter © 2008 Elsevier Inc. All rights reserved.

doi:10.1016/j.bcp.2008.07.003

unlike classical anthracyclines, is not cardiotoxic at optimal antitumor doses [3,4] and retains antitumor activity in various multidrug-resistant tumor models [1,2,5,6]. Recently, encouraging results have been obtained in Phase I/II clinical trials conducted in Europe and China, in which the drug was administered by the intra-hepatic artery route to patients with hepatocellular carcinoma [7]. Based on these clinical data and on preclinical results showing MMDX synergism with cisplatin, the MMDX-cisplatin combination is currently undergoing multicenter Phase I/II clinical trials for the loco-regional treatment of hepatocellular carcinoma in Europe.

In vivo, MMDX is 80–120-fold more potent than doxorubicin [2]. By contrast, its *in vitro* cytotoxicity is only eight- and two-fold greater than that of doxorubicin toward cultured drug-sensitive tumor cells and hematopoietic progenitor cells, respectively [3,8]. Various studies have also shown that incubation of MMDX with NADPH and isolated human, mouse or rat liver microsomes results in marked enhancement of potency toward cultured tumor cells [9–11], suggesting that MMDX is converted to a much more cytotoxic metabolite(s) by liver microsomal enzymes. Further *in vivo* [10] and *in vitro* results [9–12] suggest that enzymes belonging to the CYP3A subfamily are involved in MMDX biotransformation. A recent study from our laboratories [13] established that MMDX is converted by human liver microsomes (HLMs) to a major metabolite, identified as 3'-deamino-3'', 4'-anhydro-[2''(S)-methoxy-3''(R)-oxy-4''-morpholinyl]doxorubicin (PNU-159682) (Fig. 1). Our work also definitely showed that CYP3A4 is the CYP form responsible for PNU-159682 formation from MMDX by HLMs [13]. PNU-159682 was found to be 700–2400-fold more potent than its parent drug toward cultured human tumor cells, and exhibited significant efficacy in *in vivo* tumor models [13]. These results suggest that PNU-159682 is the chemical entity responsible for the liver microsome-mediated increase in MMDX cytotoxicity *in vitro* [9–11] and conceivably plays a dominant role in the *in vivo* antitumor activity of the drug.

Preclinical toxicity studies have shown significant sex- and species-related differences in MMDX short-term host toxicity. In particular, LD₅₀ values of MMDX (i.v. single-dose) for male and female Beagle dogs, and female Sprague-Dawley rats were two to three times higher than those observed in male Sprague-Dawley rats or CD-1 mice of either sex [4,14]. Of the possible variables contributing to inter-species differences in the efficacy/toxicity of a liver-activated anticancer prodrug,

the rate of its metabolic activation is probably the most critical. However, quantitative information is not yet available on animal MMDX conversion to PNU-159682. Therefore, the aim of the present study was to investigate and quantitatively compare MMDX metabolism by liver microsomes obtained from rats, mice, and dogs of both sexes, as well as from human beings, in order: (1) to ascertain whether PNU-159682 is also the major oxidative MMDX metabolite in currently used laboratory animals and to identify the CYP form(s) responsible for MMDX biotransformation; (2) to assess whether a relationship exists between the extent of *in vitro* PNU-159682 formation and the *in vivo* MMDX toxicity data reported in the literature for the animals tested in this study [4,14]; (3) to assess which of the investigated animal species provides the most suitable *in vitro* model for further studies of MMDX hepatic metabolism and for examining possible metabolic interactions with co-administered drugs.

2. Materials and methods

2.1. Chemical and biological materials

MMDX hydrochloride and PNU-159682 (as free base) were synthesized at Nerviano Medical Sciences S.r.l. (Nerviano, Italy). Midazolam (MDZ), 1'-hydroxy-midazolam (1'-OH-MDZ) and 4-hydroxy-midazolam (4-OH-MDZ) were kindly provided by Roche S.p.A. (Milan, Italy). Methanol and acetonitrile (all HPLC grade) were from Carlo Erba Reagenti (Milan, Italy). Ketoconazole, troleandomycin (TAO), erythromycin, dextromethorphan, dextrorphan and NADPH, as well as other chemicals, were purchased from Sigma-Aldrich Italia S.r.l. (Milan, Italy). Ultrapure water was obtained by means of a Millipore (Bedford, MA, USA) MilliQ apparatus.

MDZ was prepared daily in 50% methanol, final solvent concentration in the assay medium being 0.5%. Both ketoconazole and TAO were initially dissolved in acetonitrile and appropriate amounts (see below) were transferred to the test tube. Acetonitrile was then evaporated under a gentle stream of nitrogen before adding the other components of the incubation mixture.

Pooled, mixed-gender HLMs were provided by BD Gentest (Woburn, MA, USA). Male and female HLMs (pooled from 10 male and 10 female donors, respectively) and pooled liver

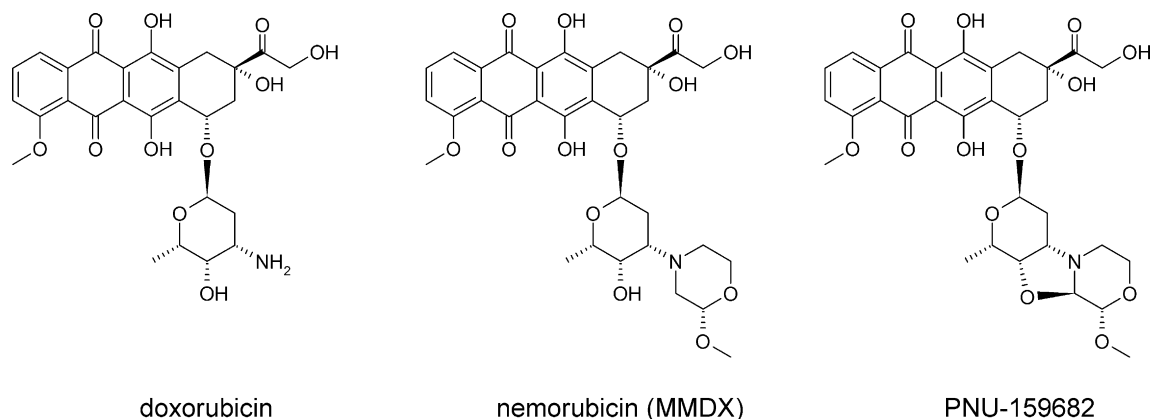


Fig. 1 – Structures of doxorubicin, nemorubicin (MMDX) and PNU-159682.

microsomes from male and female Sprague-Dawley rats, CD-1 mice, and Beagle dogs were purchased from XenoTech, LLC (Lenexa, KS, USA). Liver microsomes obtained from β -naphthoflavone (BNF)- or phenobarbital (PB)-treated male rats, mice and dogs, dexamethasone (DEX)-treated male rats and mice, and rifampin (RIF)-treated male dogs were also provided by XenoTech, LLC. All microsomal preparations were stored in aliquots at -80°C until use. The protein concentration of each microsomal preparation, CYP content, and schedules for animal treatments with CYP inducers were provided by the manufacturer.

Rabbit inhibitory anti-rat CYP3A1 antiserum and non-immune rabbit serum were also obtained from XenoTech, LLC.

2.2. Identification of PNU-159682 as a product of MMDX metabolism by animal liver microsomes

Formation of PNU-159682 from MMDX by NADPH-supplemented liver microsomes of untreated rats, mice or dogs was qualitatively assessed in the supernatant from typical incubation mixtures (see below) by means of an HPLC system consisting of a 2795 Alliance HT separation module equipped with a 2996 UV-visible photodiode array detector, and a Micromass ZQ single quadrupole mass spectrometer with an electrospray ion source (all from Waters Corp., Milford, MA, USA). Instrument control, data acquisition and data processing were performed with the Empower and MassLynx 4.0 software (Waters Corp.). Chromatographic conditions were as follows: column, Xterra RP₁₈ (4.6 mm \times 50 mm, 5 μm ; Waters Corp.); mobile phase, 5 mM ammonium acetate (pH 5.2)/acetonitrile (95:5 v/v; solvent A) and water/acetonitrile (5:95 v/v; solvent B); elution program, linear gradient from 10 to 90% solvent B from 0 to 8 min, followed by increase to 100% solvent B in 1 min; post-run time, 2 min; flow rate, 1 ml/min; injection volume, 10 μl ; column temperature, 30 $^{\circ}\text{C}$; detection, photodiode array and mass spectrometry. In the above conditions, retention times of MMDX and PNU-159682 were 4.8 and 5.4 min, respectively. The mass spectrometer operated in the following conditions: electrospray in both positive-ion (ES+) and negative-ion modes (ES-); capillary voltage, 3.5 kV (ES+) and 28 V (ES-); source temperature, 120 $^{\circ}\text{C}$; scan mode, full scan from 100 to 800 atomic mass units (amu).

2.3. Determination of initial rates of PNU-159682 formation by animal and human liver microsomes

The incubation mixture (total volume: 0.2 ml) consisted of 0.3 M Tris (pH 7.4), 0.5 mM NADPH, increasing concentrations of MMDX (from 1 to 50 μM , $n = 8$), and microsomal proteins. Results from preliminary experiments indicated that the rates of PNU-159682 formation from MMDX were linear for microsomal protein concentrations up to 0.5 mg/ml (male and female human and mouse, male rat) or 1.0 mg/ml (male and female dog, female rat), and for incubation times up to 15 min (male and female mouse), 20 min (male and female humans, male rat), and 120 min (male and female dog, female rat). Accordingly, kinetic studies were performed by incubating microsomal proteins (final concentration 0.25 mg/ml) in the above-specified mixture for 5 min (male and female mouse), 10 min (male and female humans, male rat) and 60 min (male

and female dog, female rat). Following thermal equilibration of the incubation mixtures at 37 $^{\circ}\text{C}$, reactions were started by the addition of microsomes, conducted in a shaking water bath at 37 $^{\circ}\text{C}$ in aerobic conditions, and stopped by adding 50 μl of ice-cold methanol and cooling the sample on ice. Denatured proteins were then removed by centrifugation for 20 min at 20,000 $\times g$ (4 $^{\circ}\text{C}$), and an aliquot (100 μl) of the supernatant was analyzed for PNU-159682 quantification by means of HPLC, as described below (Section 2.5).

2.4. Evaluation of the role of CYP3A enzymes in MMDX conversion to PNU-159682 by animal liver microsomes

In these experiments, the general incubation procedures were identical to those described above for kinetic studies, except that a single MMDX concentration (20 μM) was used on the basis of K_m values obtained for the various species (see Section 3). The experimental approaches used for assessing the role of CYP3A are described in detail in the following sections.

2.4.1. Chemical and immunochemical inhibition studies

The conversion of MMDX to PNU-159682 by animal and human liver microsomes was determined in the absence or presence of the selective CYP3A inhibitors ketoconazole or TAO [15–20]. Since ketoconazole, at concentrations $\leq 1 \mu\text{M}$, is a reversible inhibitor of CYP3A activities in human and dog liver microsomes [15–17], increasing amounts of this compound were directly included in the incubation mixture (final ketoconazole concentration, 0.01–1 μM , $n = 5$). By contrast, TAO, which is a quasi-irreversible inhibitor of various mammalian CYP3A enzymes, requires NADPH-dependent metabolism to form an inhibitory metabolite-CYP3A complex [18–20]. Therefore, increasing concentrations of TAO (5–100 μM , $n = 5$) were pre-incubated with liver microsomes and NADPH (0.5 mM) for 15 min at 37 $^{\circ}\text{C}$ before adding MMDX and an additional amount (0.1 μmol) of NADPH. The reactions were then conducted as described above.

Immunochemical inhibition studies were carried out with a rabbit inhibitory anti-rat CYP3A1 antiserum which, according to the manufacturer, specifically inhibits the CYP3A-mediated testosterone 6- β -hydroxylation in HLMs by >75% when used at a serum-to-microsomal protein ratio of 25 μl to 100 μg . In detail, 50 μg of microsomal protein were pre-incubated for 5 min at 37 $^{\circ}\text{C}$ in 0.3 M Tris (pH 7.4) with amounts of antiserum ranging from 1 to 12.5 μl , or an equal volume of non-immune rabbit serum (control); the reaction was then started by the addition of MMDX (final concentration, 20 μM) and NADPH (final concentration, 0.5 mM), and conducted as described above.

2.4.2. Rates of PNU-159682 formation by liver microsomes from rats, mice, and dogs treated with various CYP inducers, and correlation analysis with different CYP marker activities

PNU-159682 formation from MMDX was also evaluated using liver microsomes obtained from male rats, mice and dogs treated with CYP-inducing agents (Section 2.1). In these experiments, incubation conditions were the same as those described above for the kinetic experiments, since control experiments had indicated that PNU-159682 formation by induced liver microsomes is also linear in those conditions.

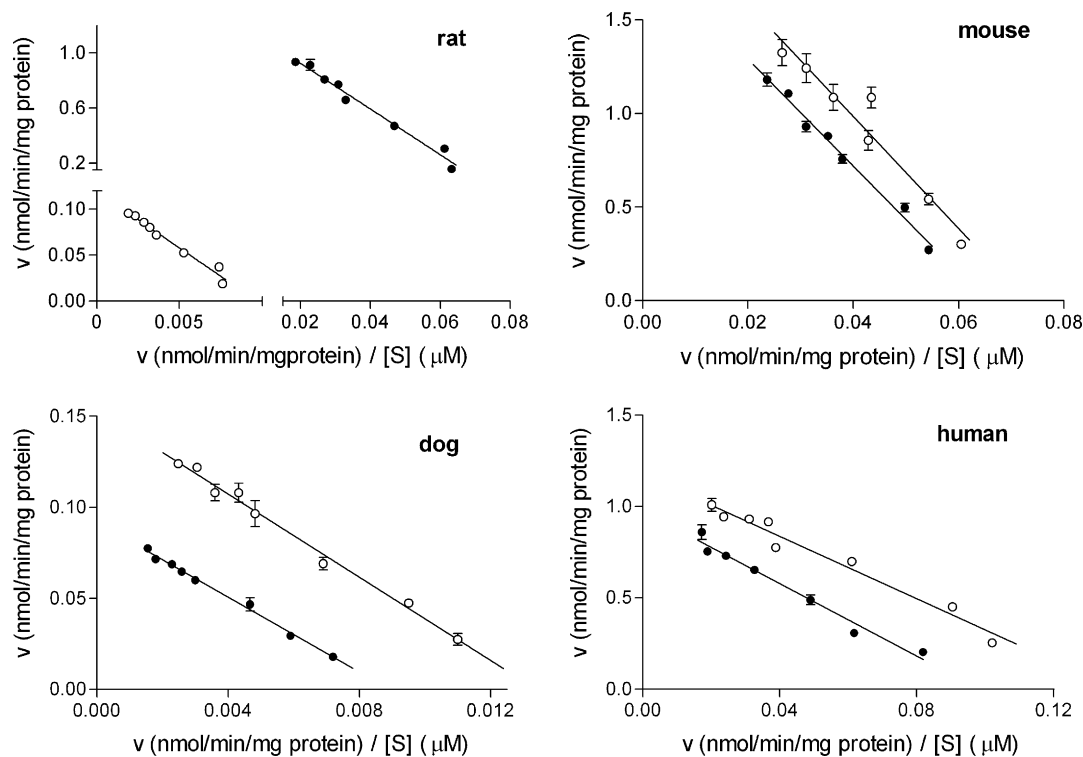


Fig. 2 – Eadie-Hofstee plots for MMDX conversion to PNU-159682 by male (●) and female (○) rat, mouse, dog and human liver microsomes. Data points are the means of three determinations. Bars represent S.E.M., they are not shown when the size of data points is larger than S.E.M. bars. Solid lines were obtained by linear regression analysis of the data.

The rates of PNU-159682 formation obtained from this set of experiments were analyzed for correlation with four established CYP marker reactions, evaluated in the same microsomal samples: MDZ 1'-hydroxylation (CYP3A [21, and references therein]); MDZ 4-hydroxylation (CYP3A [22-24]); erythromycin N-demethylation (CYP3A [25-27, and references therein]); dextrometorphan O-demethylation (CYP2D; [23,28-30]).

MDZ 1'-hydroxylation and MDZ 4-hydroxylation were simultaneously assayed in incubation mixtures (total volume: 0.2 ml) containing 0.1 M potassium phosphate buffer (pH 7.4), 25 μ M midazolam, 0.5 mM NADPH, and an appropriate amount of liver microsomes (0.1 mg/ml for rat and dog; 0.25 mg/ml for mouse). The reactions, started by the addition of the microsomes following thermal equilibration of incubation mixtures

Table 1 – Kinetic parameters for PNU-159682 formation by liver microsomes from male and female rats, mice, dogs and humans

Species and sex	K_m (μ M)	V_{max} (nmol/min/mg protein)	CL_{int} (μ l/min/mg protein)
Rat			
Male	17.05 \pm 2.61 ^a	1.267 \pm 0.070 ^a	75.11 \pm 8.96 ^b
Female	12.58 \pm 2.84	0.120 \pm 0.012 ^{***,c}	9.72 \pm 1.27 ^{***,c}
Mouse			
Male	29.44 \pm 3.97 ^c	1.876 \pm 0.150 ^c	64.18 \pm 6.11 ^c
Female	28.10 \pm 2.33 ^c	2.157 \pm 0.190 ^c	77.37 \pm 11.94 ^a
Dog			
Male	10.51 \pm 2.30	0.091 \pm 0.003 ^c	8.92 \pm 1.66 ^c
Female	12.34 \pm 2.45	0.156 \pm 0.001 ^{***,c}	12.98 \pm 2.63 ^c
Human			
Male	9.15 \pm 0.25	0.925 \pm 0.005	101.10 \pm 2.27
Female	11.75 \pm 2.97	1.288 \pm 0.146 [*]	112.40 \pm 16.54

Each value is the mean \pm S.D. of three determinations performed in duplicate. Student's t-test for unpaired data was used for statistical evaluation of differences between liver microsomes from individuals of the same species but of different sex. ^a $P < 0.05$; ^b $P < 0.01$; ^c $P < 0.001$. One-way ANOVA followed by post-hoc Tukey's multiple comparison was used to test for differences between liver microsomes from individuals of the same sex but of different species; for clarity, only symbols indicating differences between animal and human liver microsomes are shown. ^a $P < 0.05$; ^b $P < 0.01$; ^c $P < 0.001$.

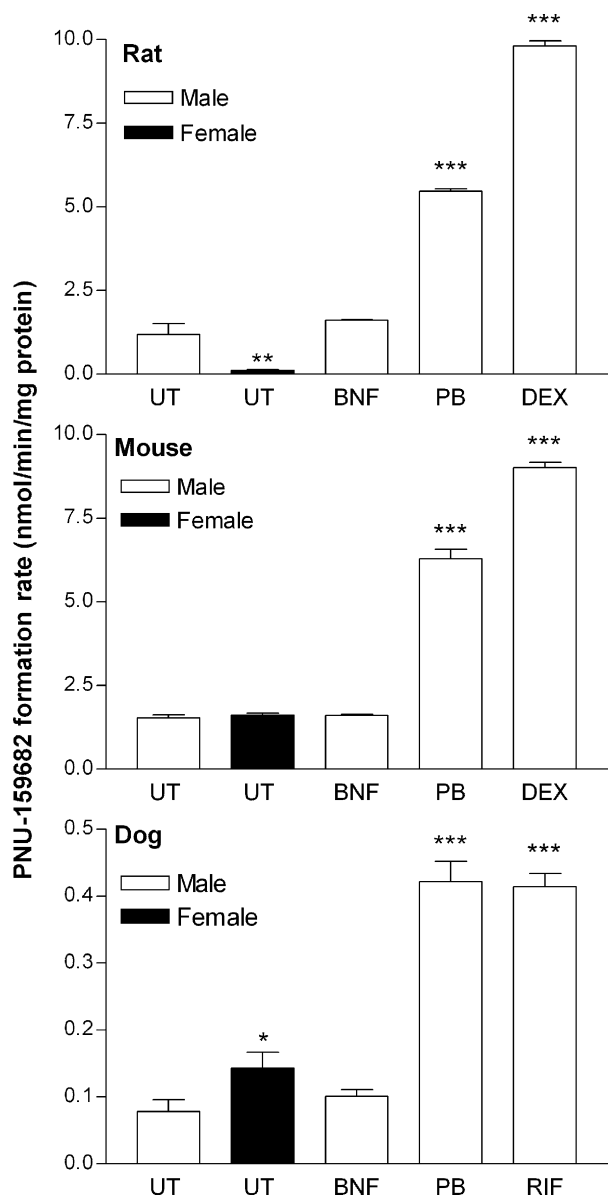


Fig. 3 – Influence of sex and pretreatment with prototypical CYP inducers on MMDX conversion to PNU-159682 by rat, mouse and dog liver microsomes. Metabolite formation was measured in linear reaction conditions at a substrate concentration of 20 μ M. Results are the means \pm S.E.M. from three experiments carried out in duplicate. UT, untreated; BNF, β -naphthoflavone, PB, phenobarbital; DEX, dexamethasone; RIF, rifampin. * $P < 0.05$, ** $P < 0.01$ and * $P < 0.001$ vs values obtained with liver microsomes from untreated male animals.**

at 37 °C, were conducted for 5 min at 37 °C and stopped by the addition of 0.1 ml of ice-cold methanol. 1'-OH-MDZ and 4-OH-MDZ formation was quantitatively evaluated in aliquots (100 μ l) of supernatants by HPLC analysis, as previously described in detail [31].

Erythromycin *N*-demethylation was determined in incubation mixtures (total volume: 0.4 ml) containing 0.1 M potassium phosphate buffer (pH 7.4), 0.5 mM erythromycin, 1 mM

NADPH, and microsomal protein (0.25 mg/ml). The reaction was conducted for 10 min at 37 °C and stopped by addition of 0.1 ml of ice-cold ethanol. An aliquot (100 μ l) of the supernatant was analyzed for formaldehyde content by an HPLC method, exactly as described by Quintieri et al. [13].

Dextromethorphan *O*-demethylation was determined in 0.1 M potassium phosphate buffer (pH 7.4) containing 20 μ M dextromethorphan, 0.5 mM NADPH, and an appropriate amount of liver microsomes (0.10 mg/ml for rat; 0.25 mg/ml for mouse and dog) in a final volume of 0.2 ml. The reaction, started by the addition of the microsomes, was stopped after 20 min (mouse and rat) or 30 min (dog) of incubation at 37 °C, by addition of 10 μ l of ice-cold 60% perchloric acid. An aliquot (100 μ l) of the supernatant was analyzed for dextrorphan formation by HPLC with UV detection, as described below.

2.5. HPLC analysis

Quantitative evaluation of PNU-159682 formation was performed by means of HPLC with UV detection in a series 1100 HPLC system equipped with solvent degasser, quaternary pump, autosampler, column oven, and multiple wavelength UV-visible detector (Agilent Technology, formerly Hewlett-Packard GMBH, Waldbronn, Germany); data were collected and integrated with Hewlett-Packard ChemStation software (version A.06.03). Chromatographic conditions were as follows: column, Symmetry C8 (4.6 mm \times 250 mm, 5 μ m; Waters Corp.); mobile phase, 10 mM ammonium acetate (pH 5.0)/methanol/acetonitrile (45:30:25 v/v/v); flow rate, 1.2 ml/min; injection volume, 100 μ l; column temperature, 30 °C; detection, UV absorbance at 254 nm. In these conditions, retention times of MMDX and PNU-159682 were 6.7 and 8.1 min, respectively. For quantitative determination of PNU-159682, calibration curves were obtained daily with authentic PNU-159682 at concentrations ranging from 0.1 to 1.0 nmol/0.2 ml ($n = 5$). The calibration curves were linear in this concentration range ($r^2 \geq 0.98$), the lowest value of the range representing the limit of quantification of the analyte. Inter- and intra-assay coefficients of variation (CV) for PNU-159682 determination ($n = 6$) were both lower than 4 and 3% at 0.1 and 1 nmol/0.2 ml, respectively.

Quantitative evaluation of dextrorphan, a product of CYP2D-mediated metabolism of dextromethorphan, was carried out with the above-described Hewlett-Packard series 1100 HPLC system. Chromatographic conditions were as follows: column, Zorbax Eclipse XDB-C8 (4.6 mm \times 150 mm, 5 μ m; Agilent Technologies, Palo Alto, CA, USA); mobile phase, 20 mM ammonium acetate (pH 4.5)/methanol (70:30, v/v; solvent A) and acetonitrile (solvent B); elution program, isocratic elution with 100% solvent A for 5 min, linear gradient elution from 0 to 15% solvent B in 10 min, followed by isocratic elution with 15% solvent B for 6 min; post-run time, 5 min; flow rate, 1.3 ml/min; injection volume, 100 μ l; column temperature, 30 °C; detection, UV absorbance at 280 nm. In the above conditions, retention times of dextrorphan and dextromethorphan were 8.3 and 18.0 min, respectively. For quantification of dextrorphan, calibration curves were obtained daily using authentic dextrorphan in the range 0.3–6.0 nmol/0.2 ml ($n = 6$). The calibration curves were linear

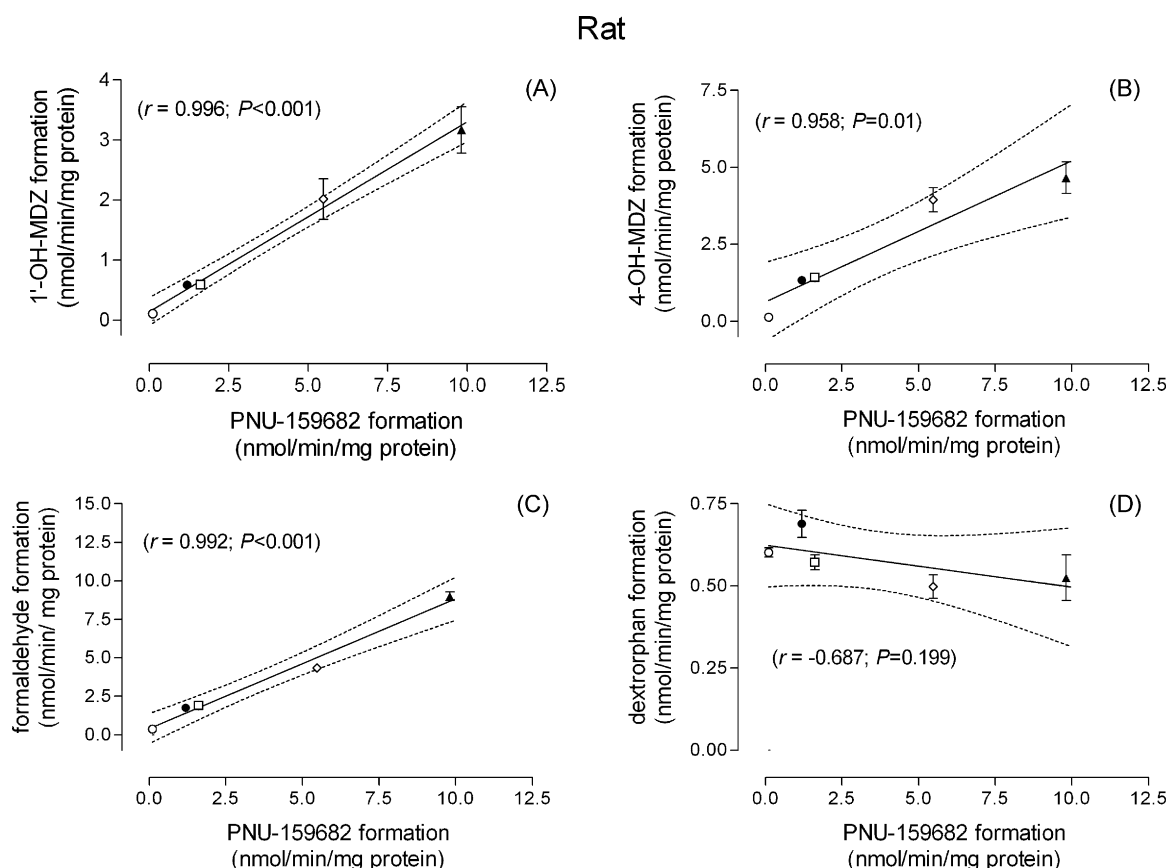


Fig. 4 – Correlation between rates of PNU-159682 formation and CYP marker activities in liver microsomes from untreated male (●) and female (○) rats and from male rats treated with β -naphthoflavone (□), phenobarbital (◇) or dexamethasone (▲). Evaluated marker activities for CYP3A were: 1'-hydroxylation of MDZ (panel A), 4-hydroxylation of MDZ (panel B), and erythromycin-N-demethylation (panel C). The CYP2D marker activity dextrometorphan-O-demethylation is reported in panel D. Protocol and assay conditions are reported in detail in Section 2. Data points represent the means \pm S.E.M. from three experiments; S.E.M. values are not shown when the size of data points is larger than the S.E.M. bar. Values of PNU-159682 formation rates are those reported in Fig. 3. Dotted lines represent the 95% CI for regression lines.

in this concentration range ($r^2 \geq 0.98$), the lowest value of the range representing the limit of quantification of the analyte. Both inter- and intra-assay CVs for dextrorphan determination ($n = 6$) were lower than 5% at 0.3 nmol/0.2 ml and lower than 2% at 6 nmol/0.2 ml.

2.6. Data analysis

Initial velocity (v) data for microsomes-catalyzed PNU-159682 formation from MMDX were evaluated by graphical analysis with the Eadie-Hofstee plot (v vs $v/[S]$), the plotting technique most sensitive to deviations from linearity [32], and by best-fitting procedures, with the one- and two-site hyperbolic Michaelis-Menten models (Eqs. (1) and (2), respectively).

$$v = \frac{V_{\max}[S]}{K_m + [S]} \quad (1)$$

$$v = \frac{V_{\max 1}[S]}{K_{m1} + [S]} + \frac{V_{\max 2}[S]}{K_{m2} + [S]} \quad (2)$$

The F-test was used to discriminate between the two models. Kinetic parameters were determined by non-linear regression analysis of untransformed data (GraphPad Prism, version 3.03, GraphPad Software Inc., San Diego, CA, USA). Estimated parameters were: V_{\max} , maximum velocity of the reaction; K_m , substrate concentration yielding 50% of V_{\max} , and CL_{int} , intrinsic metabolic clearance, calculated as V_{\max}/K_m .

Statistical analyses were performed by means of GraphPad Prism software, version 3.03. Unless otherwise stated, data are presented as arithmetic means \pm S.D. Student's t -test for unpaired data was used for statistical comparisons of data obtained from liver microsomes of individuals of different sex belonging to the same species; the one-way ANOVA, followed by Tukey's post-hoc multiple comparison test, was used for analysis of data from liver microsomes of individuals of the same sex belonging to the four examined species. When two or more treatment groups were compared with the same control, one-way ANOVA was followed by Dunnett's post-hoc test. A value of $P < 0.05$ was considered significant. Correlations between two variables

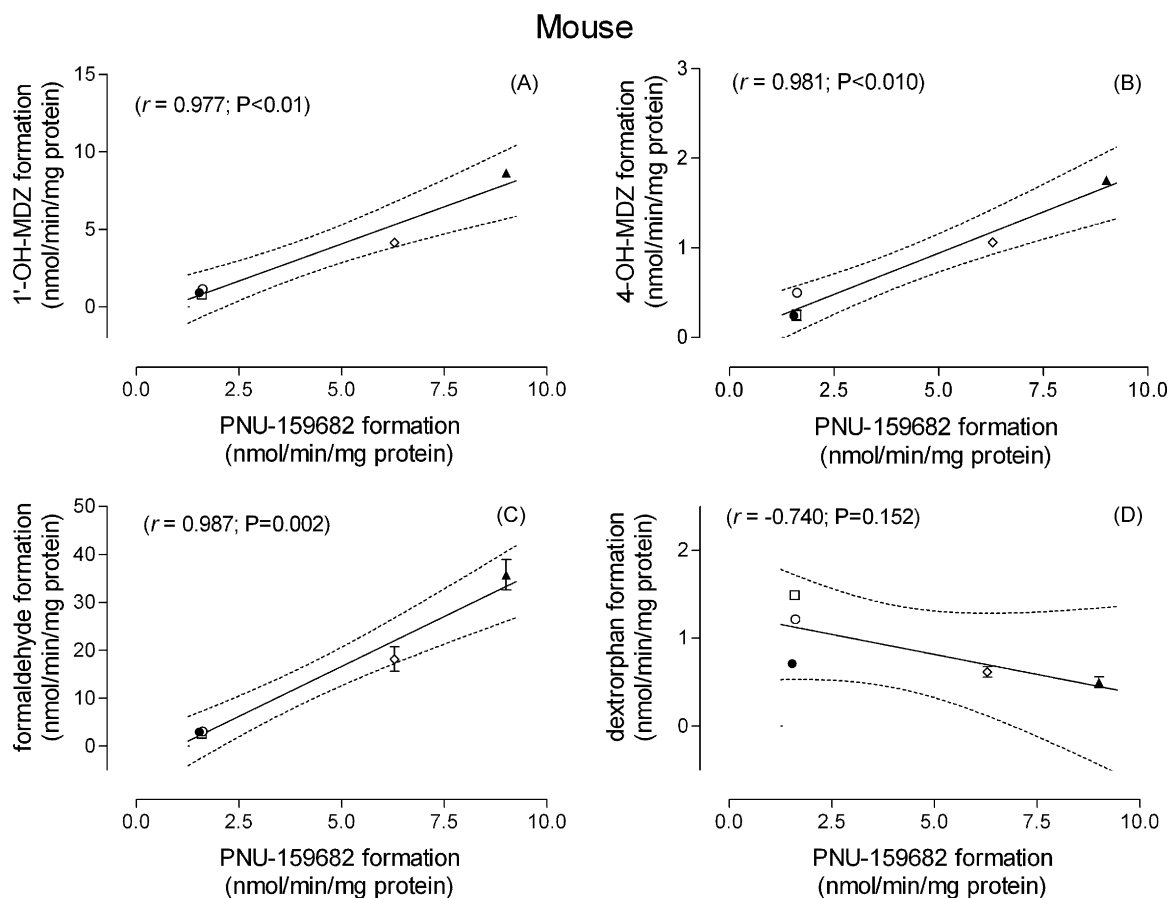


Fig. 5 – Correlation between rates of PNU-159682 formation and cyp marker activities in liver microsomes from untreated male (●) and female (○) mice and from male mice treated with β -naphthoflavone (□), phenobarbital (◇) or dexamethasone (▲). Evaluated marker activities for cyp3a and cyp2d are those indicated in the legend to Fig. 3. Data points represent the means \pm S.E.M. from three experiments; S.E.M. values are not shown when the size of data points is larger than the S.E.M. bar. Values of PNU-159682 formation are those reported in Fig. 3.

were examined by linear regression analysis (GraphPad Prism software, version 3.03).

3. Results

3.1. Identification of PNU-159682 as a major metabolic product of MMDX and kinetics of its formation by liver microsomes from male and female rats, mice, and dogs

Analysis of supernatants from experiments in which MMDX was incubated with NADPH-supplemented liver microsomes from rats, mice or dogs by HPLC coupled to photodiode array and mass spectrometric detection led to chromatograms characterized by a major metabolite peak whose retention time, UV-visible absorbance spectrum and m/z value were identical to that of synthetic PNU-159682. In all species, the PNU-159682 peak was undetectable when NADPH or liver microsomes were omitted from the incubation mixture.

PNU-159682 formation rates were then measured over a substrate concentration range of 1–50 μ M, with liver microsomes from male and female rats, mice, dogs and humans. Eadie-Hofstee plots (Fig. 2) were linear for all species.

Consistent with the results of graphical analysis, the best fit of untransformed initial velocity data was always obtained by means of the one-site Michaelis–Menten equation. These analyses indicated that a single microsomal enzyme following classical Michaelis–Menten (hyperbolic) kinetics [33] is involved in MMDX oxidation to PNU-159682. Mean values of K_m and V_{max} , calculated by means of the best-fitting procedure, and CL_{int} (V_{max}/K_m) values are summarized in Table 1. No marked sex-related differences in kinetic parameters were observed with liver microsomes from mice, whereas pronounced sexual dimorphism in MMDX metabolism was evident in the rat, PNU-159682 being formed at much lower rates by female than male rat liver microsomes. In particular, V_{max} in females was about one-tenth that observed in males, whereas K_m did not differ significantly between sexes. Consequently, MMDX CL_{int} for PNU-159682 formation was about eight-fold lower for female than male rat liver microsomes. A lesser, but statistically significant, inter-sex difference in PNU-159682 formation was also observed with dog microsomes, V_{max} being about two-fold higher for female than male liver microsomes. However, this difference did not translate into different CL_{int} values between sexes. Overall, K_m did not differ between sexes, and varied by a factor of three

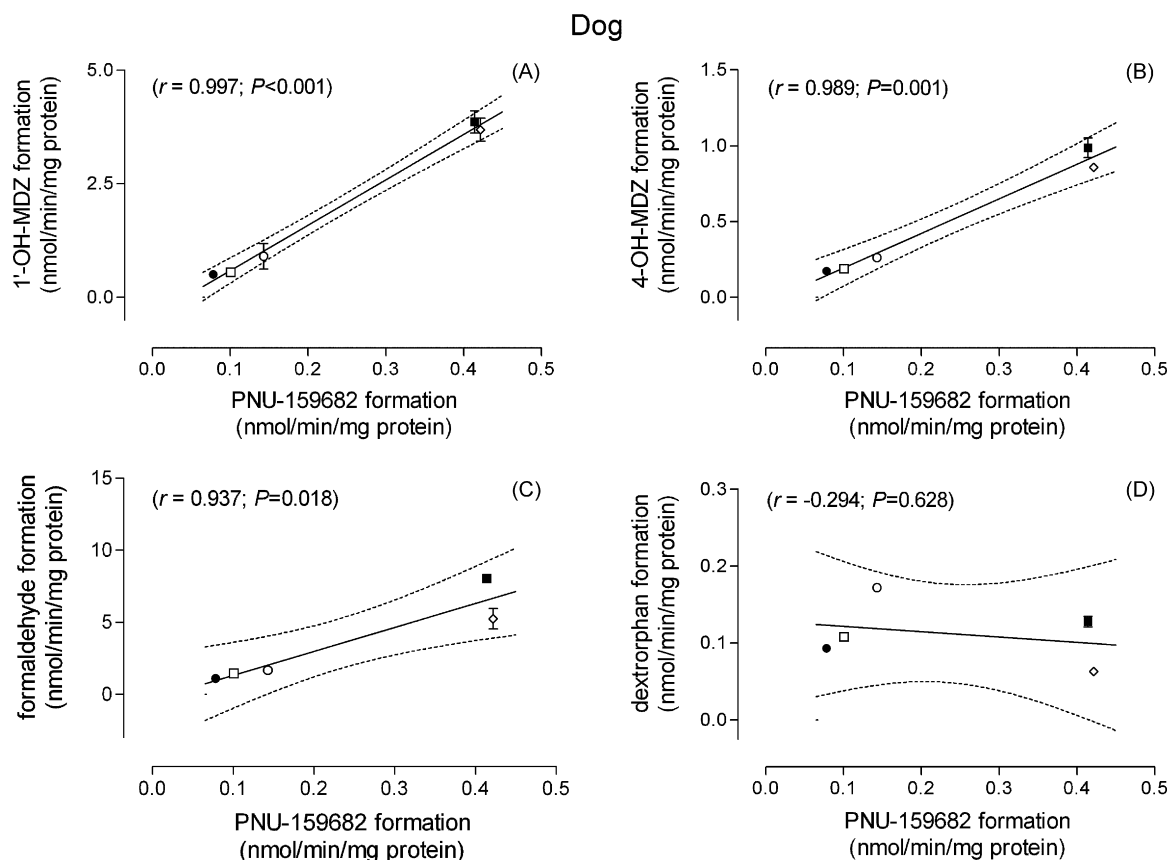


Fig. 6 – Correlation between rates of PNU-159682 formation and CYP marker activities in liver microsomes from untreated male (●) and female (○) dogs and from male dogs treated with β -naphthoflavone (□), phenobarbital (◇) or rifampin (■). Evaluated marker activities for CYP3A and CYP2D are those indicated in the legend to Fig. 4. Data points represent the means \pm S.E.M. from three experiments; S.E.M. values are not shown when the size of data points is larger than the S.E.M. bar. Values of PNU-159682 formation are those reported in Fig. 3.

among species, ranging from 9 μ M in the male human to 29 μ M in the male mouse. By contrast, V_{\max} exhibited highly significant sex-related differences in two species (rat and dog) and varied by a factor of 20 among species, ranging from 0.09 nmol/min/mg protein in the male dog to 2 nmol/min/mg protein in the female mouse. The rank order of MMDX CL_{int} was: female human \approx male human $>$ female mouse \approx male rat $>$ male mouse \gg female dog \approx female rat \approx male dog.

3.2. Involvement of CYP3A enzymes in PNU-159682 formation by rat, mouse, and dog liver microsomes

Our previous work identified CYP3A4 as the enzyme responsible for PNU-159682 formation from MMDX by HLMs [13]. In order to ascertain whether a member of the liver CYP3A subfamily also plays a predominant role in the conversion of MMDX to PNU-159682 in the investigated laboratory animal species, several experimental approaches were used.

3.2.1. Effect of various CYP inducers on PNU-159682 formation by liver microsomes from rats, mice, and dogs

A first set of experiments evaluated the rate of PNU-159682 formation from 20 μ M MMDX by liver microsomes from

untreated male and female rats, mice and dogs, and from male animals of those species treated with various prototypical CYP-inducing agents, i.e., BNF (rat, mouse and dog CYP1A; [34]), PB (rat, mouse, and dog CYP2B and 3A, and rat and mouse CYP2C; [34–36]), DEX (rat and mouse CYP2B, CYP2C and 3A; [35]), and RIF (dog CYP3A [34]). The results reported in Fig. 3 confirmed the strong sexual dimorphism in PNU-159682 formation by rat liver microsomes, as well as the less marked, but statistically significant, difference ($P < 0.05$) between male and female dogs. Pretreatment of male mice and rats with PB or DEX, but not with BNF, significantly increased ($P < 0.01$) the rate of MMDX oxidation to PNU-159682 by isolated liver microsomes, DEX being the most effective inducer. Similarly, dog pretreatment with PB or RIF significantly ($P < 0.01$) increased the rate of PNU-159682 formation, whereas BNF pretreatment did not.

3.2.2. Correlation between CYP marker activities and PNU-159682 formation rates

For these experiments, we employed the same panel of microsomes from inducer-treated and untreated males used for the above experiments, as well as liver microsomes from untreated females of each animal species. We assayed three

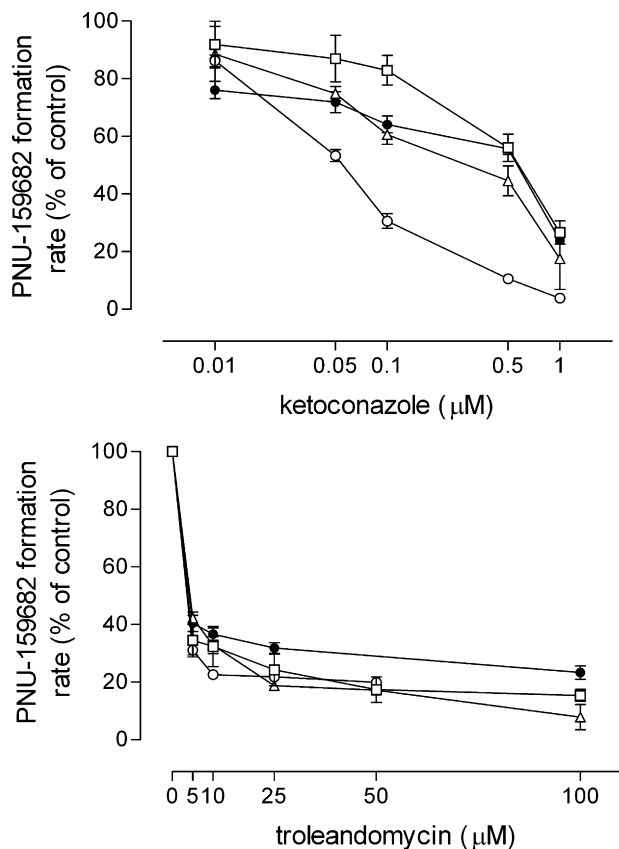


Fig. 7 – Concentration-dependent inhibitory effect of ketoconazole and troleandomycin on PNU-159682 formation rate by male rat (□), mouse (○), dog (△), and pooled, mixed-gender human (●) liver microsomes. Protocol and assay conditions are reported in detail in Section 2. Results are reported as percent of control activity. Each value is the mean \pm S.E.M. from three experiments carried out in duplicate. Mean control values (in the absence of inhibitors) for PNU-159682 formation by male rat, mouse, dog and human liver microsomes were 1.19 ± 0.32 , 1.53 ± 0.09 , 0.078 ± 0.018 , and 0.653 ± 0.01 nmol/min/mg protein, respectively.

CYP3A marker reactions: formation of 1'-OH-MDZ and 4-OH-MDZ from MDZ [21–24], and formaldehyde formation through erythromycin-N-demethylation [25–27]. We also measured dextrophan formation through dextromethorphan-O-demethylation, which is a marker reaction of enzymes belonging to the CYP2D subfamily [23,28–30]. A correlation analysis was then performed between the velocities of these marker reactions and those of PNU-159682 formation by the same microsomal preparations from rats, mice, and dogs. Figs. 4–6 show highly significant positive linear correlations (r 0.937–0.997; $P \leq 0.018$) between the formation rates of PNU-159682 and those of 1'-OH-MDZ, 4-OH-MDZ and formaldehyde (through erythromycin-N-demethylation) in all animal species. By contrast, no statistically significant correlations ($P > 0.05$) were found between PNU-159682 formation rate and dextromethorphan-O-demethylase activity (Figs. 4–6).

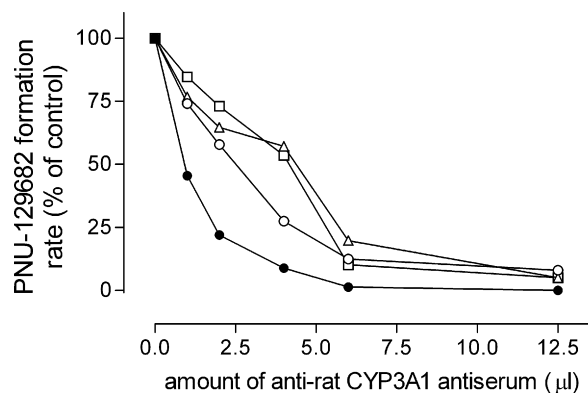


Fig. 8 – Inhibitory effect of increasing amounts of rabbit anti-rat CYP3A1 antiserum on PNU-159682 formation rate by male rat (●), mouse (□), dog (△), and pooled, mixed-gender human (○) liver microsomes. Experimental details are reported in Section 2. Results are reported as percent of control activity (in the presence of an equal volume of non-immune rabbit serum). Each point represents the mean of two separate determinations performed in duplicate.

3.2.3. Effect of chemical and immuno-chemical inhibitors on MMDX conversion to PNU-159682 by rat, mouse and dog liver microsomes

In order to confirm the above results, we examined the effects of the CYP3A inhibitors ketoconazole [15–17] and TAO [18–20] on the rate of PNU-159682 formation by microsomes obtained from males of the various animal species. For the purpose of comparison, the same experiments were also performed using pooled, mixed-gender HLMs. Both ketoconazole and TAO inhibited, in a concentration-dependent manner, PNU-159682 formation by liver microsomes from all tested animal species and HLMs (Fig. 7). Mean maximum inhibitions of PNU-159682 formation were similar in rat, mouse, dog and human microsomes: 75%, 96%, 83% and 77% for ketoconazole, and 85%, 80%, 92% and 77% for TAO, respectively. To exclude the possibility that other CYP subfamilies were involved in PNU-159682 formation by rat, mouse and dog liver microsomes, metabolite formation was also determined in the presence of inhibitors of other CYP-mediated activities. The following chemical inhibitors were examined at concentrations appropriate to cause CYP form-selective inhibition in HLMs: α -naphthoflavone (1 μ M, CYP1A2-selective [16,37]), sulfaphenazole (20 μ M, CYP2C9-selective [16]), quinidine (5 μ M, CYP2D6-selective [16]), and diethylthiocarbamate (25 μ M; CYP2A6/E1-selective [38]). They caused a $\leq 10\%$ reduction of PNU-159682 formation rate in all animal species (data not shown). Therefore, according to the criteria of Bogaards et al. [39], they were not considered inhibitors of PNU-159682 formation catalyzed by rat, mouse or dog liver microsomes.

Consistent with these results, an anti-rat CYP3A1 polyclonal antibody, which exhibits selective inhibition of CYP3A4-dependent testosterone 6 β -hydroxylation in HLMs (see Section 2.4.1), decreased in a concentration-dependent manner the rate of PNU-159682 formation by microsomes from all tested species (Fig. 8). As expected, the most marked inhibitory effect was observed with rat liver microsomes, 1 μ l

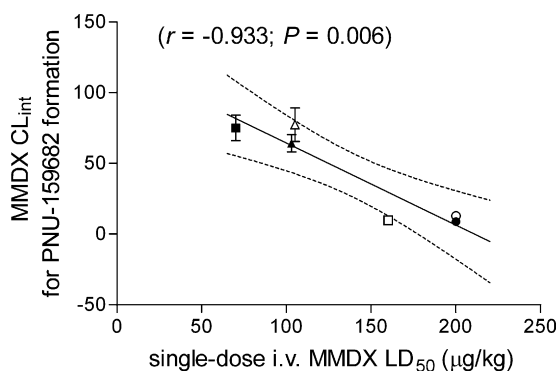


Fig. 9 – Correlation between *in vitro*-estimated CL_{int} for PNU-159682 formation and LD_{50} values of MMDX in male and female rats, mice and dogs. The values of CL_{int} are those reported in Table 1 and represent the means from three determinations carried out in duplicate. Bars represent S.D. values; they are not shown when the size of data points is larger than the S.D. bar. LD_{50} values were obtained from the literature [4,14]. (■) male rat; (□) female rat; (▲) male mouse; (△) female mouse; (●) male dog; (○) female dog. Dotted lines represent the 95% CI for regression line.

of antiserum causing about 55% inhibition of MMDX metabolism. Higher amounts of antibodies were required to inhibit PNU-159682 formation by mouse, dog and human liver microsomes to a similar extent, but very similar maximum inhibitions were obtained with all microsomal preparations.

3.3. Correlation between *in vitro*-estimated hepatic CL_{int} for MMDX conversion to PNU-159682 and *in vivo* LD_{50} of MMDX

In an attempt to explain previous observations that dogs and female rats are less susceptible than mice (of both sexes) and male rats to acute MMDX toxicity [4,14], the estimates of MMDX CL_{int} obtained in male and female rat, mouse and dog liver microsomes were analyzed for possible correlations with literature data on MMDX LD_{50} (single-dose *i.v.*) in animals of the same species, sex and strain [4,14]. A close inverse relationship ($r = -0.936$; $P = 0.006$) was found between LD_{50} and CL_{int} values (Fig. 9), strongly suggesting a role of PNU-159682 formation in the host toxicity of MMDX.

4. Discussion

In a previous work [13], we demonstrated that HLMs convert MMDX to a major, highly cytotoxic, pharmacologically active metabolite, PNU-159682 (Fig. 1) and that CYP3A4 is responsible for this biotransformation. The present work demonstrates that PNU-159682 is also a major product of MMDX metabolism by rat, mouse and dog liver microsomes, as analysis of incubation mixtures by HPLC, coupled with photodiode array and mass spectrometric detection, yielded a major metabolite peak, with retention time, UV-visible absorbance spectrum and m/z value all identical to those of authentic PNU-159682.

As previously observed with HLMs [13], a single enzyme belonging to the CYP3A subfamily is also involved in PNU-159682 formation by liver microsomes from each of the tested animal species, since: (a) both best-fitting procedures and graphical analysis of initial rate kinetics for PNU-159682 formation yielded results consistent with the single-enzyme Michaelis–Menten model; (b) the rate of PNU-159682 formation was dramatically increased by inducers of the CYP3A subfamily; (c) in all animal species, the CYP3A inhibitors ketoconazole and TAO, as well as an anti-rat CYP3A1 antiserum, caused a concentration-dependent inhibition of PNU-159682 formation, whereas selective inhibitors of five other human CYP forms (1A2, 2C9, 2D6, 2A6, 2E1) had no effect; (d) experiments including microsomes from male and female untreated animals and male animals treated with different CYP inducers showed that the rates of PNU-159682 formation are highly correlated to those of three CYP3A marker reactions (MDZ 1'-hydroxylation and 4-hydroxylation, and erythromycin-*N*-demethylation), whereas no correlation exists between PNU-159682 formation rates and those of the CYP2D marker reaction dextromethorphan-*O*-demethylation.

Correlation analyses are widely used in phenotyping reactions carried out with HLMs, for which a panel of microsomes obtained from differing subjects is necessary [40,41]. The present work indicates that this approach may be successfully used also for metabolic studies with microsomes from laboratory animal species.

The marked sexual dimorphism observed in rats for PNU-159682 formation rate, which was 10 times greater in males than in females, is a further observation supporting the important role played by the CYP3A subfamily in MMDX conversion to PNU-159682, since significantly higher expression [42] or activity [43–45] of members of the CYP3A subfamily have been consistently observed in the male. Moreover, a major role of CYP3A in PNU-159682 formation in the rat is also consistent with the previous observation by Baldwin et al. [11] that potentiation of *in vitro* MMDX cytotoxicity is achieved by co-incubating MMDX with NADPH-supplemented liver microsomes from male but not from female rats.

Since PNU-159682 is an important oxidative metabolite of MMDX, the CL_{int} of MMDX conversion to PNU-159682 may represent an index of liver efficiency in producing the metabolite mainly responsible for the *in vivo* activity of MMDX [10,13]. This role is supported by our observation of a highly significant inverse correlation between CL_{int} for its formation and reported MMDX LD_{50} values for animals of the species, sex and strains tested here [4,14]. Thus, the present study is the first to demonstrate that a close relationship exists between the *in vitro* oxidative metabolism and *in vivo* host toxicity of MMDX.

Lastly, our results give useful information on the *in vitro* animal model closest to human beings with regard to MMDX hepatic oxidative metabolism. Although qualitatively similar metabolite profiles were observed upon incubation of the drug with liver microsomes from rats, mice and dogs (present paper) as well as humans [13], striking quantitative differences were observed between species. On the basis of the V_{max} and CL_{int} values, mice of either sex and the male rat seem the laboratory animal species most similar to human beings with regard to the efficiency of MMDX metabolism to PNU-159682.

In conclusion, this study shows that *in vitro* MMDX biotransformation by liver microsomes from laboratory animals is qualitatively similar to that observed with HLMS [13], although quantitative inter-species differences exist. These conclusions are based on the following findings: (1) as previously observed with HLMS [13], PNU-159682 is a major product of MMDX metabolism by rat, mouse and dog liver microsomes; (2) a single CYP form belonging to the CYP3A subfamily is responsible for PNU-159682 formation in both humans [14] and the tested animal species; (3) there are striking sex- and species-related differences in the rate of PNU-159682 formation, the highest metabolic activity being exhibited by mice and male rats and the lowest by dogs and female rats; (4) on the basis of the kinetic parameters for PNU-159682 formation, mice of either sex and the male rat appear to provide the most suitable *in vitro* animal model for further studies of MMDX biotransformation and the evaluation of its potential for metabolic interactions with other drugs. A further important finding is the observation of a close inverse correlation between *in vitro* CL_{int} for PNU-159682 formation and MMDX single-dose *i.v.* LD_{50} values reported in the literature [4,14], indicating that differences in the extent of PNU-159682 formation are most probably responsible for the previously reported intra- and inter-species variability in acute MMDX *in vivo* host toxicity [4,14].

Acknowledgments

This work was supported by a grant from the University of Padova, Italy. We thank Dr. Rosangela Battaglia for helpful discussions. We are also grateful to Mr. Paolo Favero for helpful technical assistance.

REFERENCES

- Grandi M, Pezzoni G, Ballinari D, Capolongo L, Suarato A, Bargiotti A, et al. Novel anthracycline analogues. *Cancer Treat Rev* 1990;17:133-8.
- Ripamonti M, Pezzoni G, Pesenti E, Pastori A, Farao M, Bargiotti A, et al. *In vivo* anti-tumour activity of FCE 23762, a methoxymorpholinyl derivative of doxorubicin active on doxorubicin-resistant tumour cells. *Br J Cancer* 1992;65:703-7.
- Danesi R, Agen C, Grandi M, Nardini V, Bevilacqua G, Del Tacca M. 3'-Deamino-3'-(2-methoxy-4-morpholinyl)-doxorubicin (FCE 23762): a new anthracycline derivative with enhanced cytotoxicity and reduced cardiotoxicity. *Eur J Cancer* 1993;29A:1560-5.
- Mazué G, Iatropoulos M, Imondi A, Castellino S, Brughera M, Podestà A, et al. Anthracyclines: a review of general and special toxicity studies. *Int J Oncol* 1995;7:713-26.
- Mariani M, Capolongo L, Suarato A, Bargiotti A, Mongelli N, Grandi M, et al. Growth-inhibitory properties of novel anthracyclines in human leukemic cell lines expressing either Pgp-MDR or at-MDR. *Invest New Drugs* 1994;12:93-7.
- Bakker M, Renes J, Groenhuijzen A, Visser P, Timmer-Bosscha H, Müller M, et al. Mechanisms for high methoxymorpholino doxorubicin cytotoxicity in doxorubicin-resistant tumor cell lines. *Int J Cancer* 1997;73:362-6.
- Sessa C, Valota O, Geroni C. Ongoing phase I and II studies of novel anthracyclines. *Cardiovasc Toxicol* 2007;7:75-9.
- Ghielmini M, Colli E, Bosshard G, Pennella G, Geroni C, Torri V, et al. Hematotoxicity on human bone marrow- and umbilical cord blood-derived progenitor cells and *in vitro* therapeutic index of methoxymorpholinyl doxorubicin and its metabolites. *Cancer Chemother Pharmacol* 1998;42:235-40.
- Lau DH, Duran GE, Lewis AD, Sikic BI. Metabolic conversion of methoxymorpholinyl doxorubicin: from a DNA strand breaker to a DNA cross-linker. *Br J Cancer* 1994;70:79-84.
- Quintieri L, Rosato A, Napoli E, Sola F, Geroni G, Floreani M, et al. *In vivo* antitumor activity and host toxicity of methoxymorpholinyl doxorubicin: role of cytochrome P450 3A. *Cancer Res* 2000;60:3232-8.
- Baldwin A, Huang Z, Jounaidi Y, Waxman DJ. Identification of novel enzyme-prodrug combinations for use in cytochrome P450-based gene therapy for cancer. *Arch Biochem Biophys* 2003;409:197-206.
- Lu H, Waxman DJ. Antitumor activity of methoxymorpholinyl doxorubicin: potentiation by cytochrome P450 3A metabolism. *Mol Pharmacol* 2005;67:212-9.
- Quintieri L, Geroni C, Fantin M, Battaglia R, Rosato A, Speed W, et al. Formation and antitumor activity of PNU-159682, a major metabolite of nemorubicin in human liver microsomes. *Clin Cancer Res* 2005;11:1608-17.
- Vasey PA, Bissett D, Strolin-Benedetti M, Poggesi I, Breda M, Adams L, et al. Phase I clinical and pharmacokinetic study of 3-deamino-3-(2-methoxy-4-morpholinyl)doxorubicin (FCE 23762). *Cancer Res* 1995;55:2090-6.
- Baldwin SJ, Bloomer JC, Smith GJ, Ayrton AD, Clarke SE, Chenery RJ. Ketoconazole and sulphaphenazole as the respective selective inhibitors of P4503A and 2C9. *Xenobiotica* 1995;25:261-70.
- Newton DJ, Wang RW, Lu AY. Cytochrome P450 inhibitors. Evaluation of specificities in the *in vitro* metabolism of therapeutic agents by human liver microsomes. *Drug Metab Dispos* 1995;23:154-8.
- Lu P, Singh SB, Carr BA, Fang Y, Xiang CD, Rushmore TH, et al. Selective inhibition of dog hepatic CYP2B11 and CYP3A12. *J Pharmacol Exp Ther* 2005;313:518-28.
- Delaforge M, Jaouen M, Mansuy D. The cytochrome P-450 metabolite complex derived from troleandomycin: properties *in vitro* and stability *in vivo*. *Chem Biol Interact* 1984;51:371-6.
- Ciaccio PJ, Halpert JR. Characterization of a phenobarbital-inducible dog liver cytochrome P450 structurally related to rat and human enzymes of the P450III_A (steroid-inducible) gene subfamily. *Arch Biochem Biophys* 1989;271:284-99.
- Chang TK, Gonzalez FJ, Waxman DJ. Evaluation of triacetyloleandomycin, alpha-naphthoflavone and diethyldithiocarbamate as selective chemical probes for inhibition of human cytochromes P450. *Arch Biochem Biophys* 1994;311:437-42.
- Yuan R, Madani S, Wei XX, Reynolds K, Huang SM. Evaluation of cytochrome P450 probe substrates commonly used by the pharmaceutical industry to study *in vitro* drug interactions. *Drug Metab Dispos* 2002;30:1311-9.
- Perloff MD, von Moltke LL, Court MH, Kotegawa T, Shader RI, Greenblatt DJ. Midazolam and triazolam biotransformation in mouse and human liver microsomes: relative contribution of CYP3A and CYP2C isoforms. *J Pharmacol Exp Ther* 2000;292:618-28.
- Kobayashi K, Urashima K, Shimada N, Chiba K. Substrate specificity for rat cytochrome P450 (CYP) isoforms: screening with cDNA-expressed systems of the rat. *Biochem Pharmacol* 2002;63:889-96.

- [24] Kotegawa T, Laurijssens BE, Von Moltke LL, Cotreau MM, Perloff MD, Venkatakrishnan K, et al. In vitro, pharmacokinetic, and pharmacodynamic interactions of ketoconazole and midazolam in the rat. *J Pharmacol Exp Ther* 2002;302:1228-37.
- [25] Watkins PB, Murray SA, Winkelman LG, Heuman DM, Wrighton SA, Guzelian PS. Erythromycin breath test as an assay of glucocorticoid-inducible liver cytochromes P-450. *Studies in rats and patients. J Clin Invest* 1989;83:688-97.
- [26] Lown K, Kolars J, Turgeon K, Merion R, Wrighton SA, Watkins PB. The erythromycin breath test selectively measures P450IIIa in patients with severe liver disease. *Clin Pharmacol Ther* 1992;51:229-38.
- [27] Born SL, Fraser DJ, Harlow GR, Halpert JR. *Escherichia coli* expression and substrate specificities of canine cytochrome P450 3A12 and rabbit cytochrome P450 3A6. *J Pharmacol Exp Ther* 1996;278:957-63.
- [28] Kerry NL, Somogyi AA, Bochner F, Mikus G. The role of CYP2D6 in primary and secondary oxidative metabolism of dextromethorphan: in vitro studies using human liver microsomes. *Br J Clin Pharmacol* 1994;38:243-8.
- [29] Di Marco A, Yao D, Laufer R. Demethylation of radiolabelled dextromethorphan in rat microsomes and intact hepatocytes. *Eur J Biochem* 2003;270:3768-77.
- [30] Shou M, Norcross R, Sandig G, Lu P, Li Y, Lin Y, et al. Substrate specificity and kinetic properties of seven heterologously expressed dog cytochromes P450. *Drug Metab Dispos* 2003;31:1161-9.
- [31] Quintieri L, Palatini P, Nassi A, Ruzza P, Floreani M. Flavonoids diosmetin and luteolin inhibit midazolam metabolism by human liver microsomes and recombinant CYP 3A4 and CYP3A5 enzymes. *Biochem Pharmacol* 2008;75:1426-37.
- [32] Segel JH. *Enzyme Kinetics*. John Wiley & Sons; 1975.
- [33] Venkatakrishnan K, Von Moltke LL, Greenblatt DJ. Human drug metabolism and the cytochromes P450: application and relevance of in vitro models. *J Clin Pharmacol* 2001;41:1149-79.
- [34] Graham RA, Downey A, Mudra D, Krueger L, Carroll K, Chengelis C, et al. In vivo and in vitro induction of cytochrome P450 enzymes in beagle dogs. *Drug Metab Dispos* 2002;30:1206-13.
- [35] Corcos L. Phenobarbital and dexamethasone induce expression of cytochrome P-450 genes from subfamilies IIB, IIC, and IIIA in mouse liver. *Drug Metab Dispos* 1992;20:797-801.
- [36] Murayama N, Shimada M, Yamazoe Y, Sogawa K, Nakayama K, Fujii-Kuriyama Y, et al. Distinct effects of phenobarbital and its N-methylated derivative on liver cytochrome P450 induction. *Arch Biochem Biophys* 1996;328:184-92.
- [37] Ono S, Hatanaka T, Hotta H, Satoh T, Gonzalez FJ, Tsutsui M. Specificity of substrate and inhibitor probes for cytochrome P450s: evaluation of in vitro metabolism using cDNA-expressed human P450s and human liver microsomes. *Xenobiotica* 1996;26:681-93.
- [38] Hickman D, Wang JP, Wang Y, Unadkat JD. Evaluation of the selectivity of in vitro probes and suitability of organic solvents for the measurement of human cytochrome P450 monooxygenase activities. *Drug Metab Dispos* 1998;26:207-15.
- [39] Bogaards JJ, Bertrand M, Jackson P, Oudshoorn MJ, Weaver RJ, van Bladeren PJ, et al. Determining the best animal model for human cytochrome P450 activities: a comparison of mouse, rat, rabbit, dog, micropig, monkey and man. *Xenobiotica* 2000;30:1131-52.
- [40] Guengerich FP, Shimada T. Oxidation of toxic and carcinogenic chemicals by human cytochrome P-450 enzymes. *Chem Res Toxicol* 1991;4:391-407.
- [41] Lu AY, Wang RW, Lin JH. Cytochrome P450 in vitro reaction phenotyping: a re-evaluation of approaches used for P450 isoform identification. *Drug Metab Dispos* 2003;31:345-50.
- [42] Kawai M, Bandiera SM, Chang TK, Bellward GD. Growth hormone regulation and developmental expression of rat hepatic CYP3A18, CYP3A9, and CYP3A2. *Biochem Pharmacol* 2000;59:1277-87.
- [43] Cooper KO, Reik LM, Jayyosi Z, Bandiera S, Kelley M, Ryan DE, et al. Regulation of two members of the steroid-inducible cytochrome P450 subfamily (3A) in rats. *Arch Biochem Biophys* 1993;301:345-54.
- [44] Mahnke A, Strotkamp D, Roos PH, Hanstein WG, Chabot GG, Nef P. Expression and inducibility of cytochrome P450 3A9 (CYP3A9) and other members of the CYP3A subfamily in rat liver. *Arch Biochem Biophys* 1997;337:62-8.
- [45] Mugford CA, Kedderis GL. Sex-dependent metabolism of xenobiotics. *Drug Metab Rev* 1998;30:441-98.